Inorg. Chem. **2005**, *44*, 7328–7332

Chemistry of Transition-Metal Clusters with Mixed Sb/S Ligands: Evidence for a Terminal Sb═S Double Bond in $Cp^*_3Rh_3Sb_2S_5$ ($Cp^* = C_5Me_5$)

Andreas Lange,[†] Marek M. Kubicki,[‡] Joachim Wachter,*[,†] and Manfred Zabel[†]

Institut für Anorganische Chemie, Universität Regensburg, D-93040 Regensburg, Germany, and Laboratoire de Synthèse et d'Electrosynthèse Organométalliques, UMR5188, Université de Bourgogne, F-21078 Dijon, France

Received April 4, 2005

The reaction of $[Cp_2^*Rh_2Cl_4]$ ($Cp^* = C_5Me_5$) with a slight excess of K_3SbS_3 in boiling THF gave the neutral clusters $[Cp^*_4Rh_4S_5]$ (**1**), $[Cp^*_3Rh_3Sb_2S_5]$ (**2**), and after salt metathesis $[Cp^*_3Rh_3SbS_n]PF_6$ (**3**; $n = 5$ and 6). The structures of **1**–**3** are heterocubane clusters with Cp*Rh, S, and Sb vertices but with sulfur inserted into one (**1** and **2**) or two (**3**) edges. X-ray diffraction analysis of **2** additionally reveals a very short Sb–S distance of 2.297(1) Å within the novel μ_3-Sb_2S_4 ligand. Density functional theory calculation of the model compounds $[SSbS]^{3-}$, $[HSSbS]^{2-}$, and $[HSSbH_2S]^0$ provided strong evidence for the existence of a stable terminal Sb═S double bond in **2**.

Introduction

Multiple bonds between two different heavy main group elements are a continuous challenge for preparative and theoretical chemistry.[1] Examples of compounds with group 15(E)/16(X) element multiple bonds comprise triorganyl pnictogenide−chalcogenides of type $R_3E{=}X$[1,2] and transition-metal complexes with μ_3-EX (E = P, As; X = O, S, Se)[3] or terminal EX (E = P; X = O, S)[4] ligands. Conventional synthetic methods include the oxidative addition of the chalcogen X at the E atom of the substrate, with the stability of the resulting E−X bond decreasing as the size of elements E and X increases.[2] By contrast, the synthesis of compounds containing a Sb═S double bond seems to be more laborious.[5] During our attempts to stabilize Sb/S species within the coordination sphere of transition metals,[6] we have succeeded in realizing a π coordination of $[\mu,\eta^{2:2}\text{-SbS}]^+$ in a dimolybdenum complex.[7] In this work, we report on the synthesis and characterization of a trirhodium cluster containing a novel triply bridging Sb_2S_4 ligand that bears on one Sb vertex a terminally bound sulfur atom.

Scheme 1

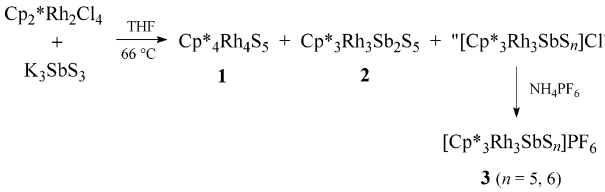

Results and Discussion

The reaction of $[Cp_2^*Rh_2Cl_4]$ with a slight excess of K_3SbS_3 (with respect to the ratio K/Cl) in boiling THF gave after chromatography dark red $[Cp^*_4Rh_4S_5]$ (**1**) and dark brown $[Cp^*_3Rh_3Sb_2S_5]$ (**2**) in yields of 10 and 7%, respectively. Alternatively, extraction of the reaction mixture with Et_2O gave soluble **1** in 24% yield along with **2** (1%) and insoluble "$[Cp^*_3Rh_3SbS_n]Cl$" ($n = 5$ and 6). This residue was dissolved in aqueous ethanol and transferred into the red salt **3** by salt metathesis with NH_4PF_6 (Scheme 1). Compound **3**, which decomposes rapidly in halogenated solvents, was further purified by filtration over silica gel.

* To whom correspondence should be addressed. E-mail: joachim.wachter@chemie.uni-regensburg.de (J.W.), marek.kubicki@u-bourgogne.fr (M.M.K.).
† Universität Regensburg.
‡ Université de Bourgogne.

(1) Power, P. P. *Chem. Rev.* **1999**, *99*, 3463−3503.
(2) Briand, G. G.; Chivers, T.; Parvez, M. *J. Chem. Soc., Dalton Trans.* **2002**, 3785−3786 and references cited therein.
(3) Scherer, O. J.; Weigel, S.; Wolmershäuser, G. *Heteroat. Chem.* **1999**, *10*, 622−626.
(4) Cummins, C. C. *Chem. Commun.* **1998**, 1777−1786.
(5) Tokitoh, N.; Arai, Y.; Sasamori, T.; Takeda, N.; Okazaki, R. *Heteroat. Chem.* **2001**, *12*, 244−249.
(6) Brunner, H.; Lange, A.; Wachter, J.; Zabel, M. *J. Organomet. Chem.* **2003**, *665*, 214−217.
(7) Brunner, H.; Kubicki, M. M.; Lange, A.; Wachter, J.; Vigier, E.; Zabel, M. *Angew. Chem., Int. Ed.* **2003**, *42*, 3547−3549.

10.1021/ic050493e CCC: $30.25
Published on Web 08/26/2005

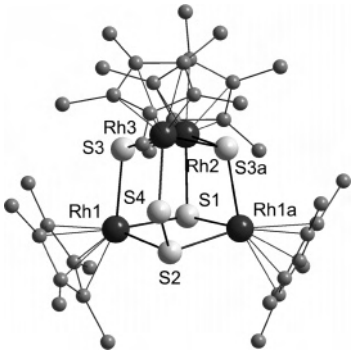

Figure 1. Structure of $[Cp^*_4Rh_4(\mu_3\text{-}S)_3(\mu_3,\eta^{1:2}\text{-}S_2)]$ (**1**). Only one molecule of the asymmetric unit is shown, whereas in the second one, the disulfide moiety (S2 and S4) is severely disordered.

The composition of **1** and **2** was confirmed by mass spectrometry, elemental analysis, and after recrystallization from toluene (**1**) or THF (**2**) by single-crystal X-ray diffraction analysis. Compound **3** may be formulated as the salt $[Cp^*_3Rh_3SbS_6]PF_6$, contaminated by $[Cp^*_3Rh_3SbS_5]PF_6$. This follows from positive electrospray ionization mass spectrometry (ESI-MS), which exhibits corresponding peaks at $m/z = 1029.0$ and 997.0, and elemental analysis.

The IR spectra of **1**−**3** reveal the typical absorptions for the Cp* ligand. The spectrum of **2** exhibits an additional weak absorption at 405 cm^{-1}, which is tentatively assigned to a ν(Sb−S) vibration. For the model compound $[HSSbH_2S]^0$ (see below), a ν(Sb═S) frequency of 416 cm^{-1} was calculated. The spectrum of **3** shows a strong absorption at 845 cm^{-1} typical of the PF_6^- anion.

The ^{1}H NMR spectrum of **1** in C_6D_6 shows three singlets at $\delta = 1.81$, 1.72, and 1.67 ppm. Their ratio 1:2:1 is consistent with the molecular structure (Figure 1), which contains two equivalent Cp*Rh1 and Cp*Rh1A moieties. Another resonance signal appears at $\delta = 1.73$ ppm in an intensity lower than that of one Cp* ligand. This signal seems to be invariant, and it cannot be removed by chromatography or crystallization. Therefore, we suppose a compound like $[Cp^*_4Rh_4S_4]$ as an impurity, which does not affect elemental analysis considerably. The ^{1}H NMR spectrum of **2** in C_6D_6 exhibits two singlets at $\delta = 1.69$ and 1.33 ppm in a 2:1 ratio. This is consistent with the molecular structure (Figure 2), which contains a mirror plane through Rh1, Sb2, S4, Sb1, S5, and S3. We were unable to record the ^{1}H NMR spectra of **3** because it decomposed in all solvents. Solutions of **1** and **2** in CD_2Cl_2 also decomposed.

Complex **1** crystallizes in the space group $P2_1/m$ with two formula units in the unit cell. Each asymmetric unit contains a pair of tetrarhodium clusters along with one toluene molecule. One molecule of each pair may properly be described by a distorted Rh_4S_4 cube, with the fifth sulfur atom (S4) being inserted into the Rh3−S2 edge (Figure 1). The atoms Rh2, Rh3, S1, S2, and S4 lie within a mirror plane. The structure of the second molecule also reveals a Rh_4S_4 core but with a severe disorder of both sulfur atoms within the disulfide moiety. Thus, despite apparently acceptable values of R1 (0.0449) and wR2 (0.0980) factors, a more detailed discussion of the structure does not make sense.

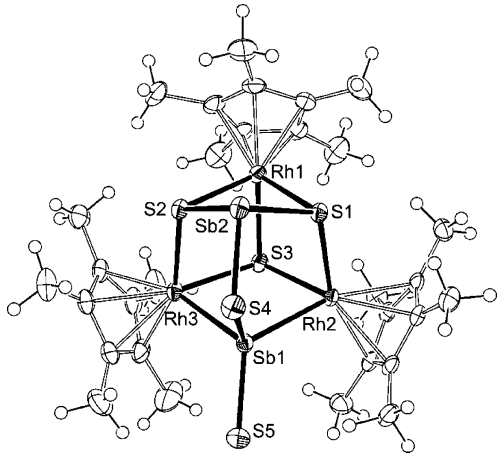

Figure 2. Structure of $[Cp^*_3Rh_3(\mu_3\text{-}S)(\mu_3\text{-}Sb_2S_4)]$ (**2**).

Chart 1. Formal Structural Relationship between Edge-Bridged Heterocubane Clusters Composed of Cp*M (M = Co, Rh), Sulfur, and Antimony Vertices

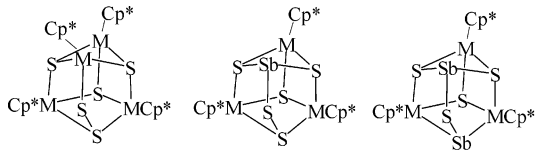

$Cp^*_4M_4S_5$ $[Cp^*_3M_3SbS_5]^+$ $[Cp^*_3M_3Sb_2S_4]^{2+}$

Complex **1** is a homologue of $[(C_5H_5)_4Co_4(\mu_3\text{-}S)(\mu_3\text{-}S_2)]$.[8] Insertion of sulfur into more cobalt−sulfur edges has been realized.[9] Examples of d^9 metal clusters with the M_4S_4 core are $[(C_5H_5)_4Co_4S_4]$[10] or $[Cp^*_4Ir_4S_4]$.[11] The corresponding rhodium cluster $[Cp^*_4Rh_4S_4]$ has been described several times, but there is no structural description thus far.[12] Representatives of the heavier homologues Se and Te are known, i.e., $[Cp^*_4Rh_4Se_4]$, $[Cp^*_4Rh_4Te_4]$, $[Cp^*_4Ir_4Se_4]$, or $[Cp^*_4Ir_4Te_4]$.[13]

The structure of **3** may be deduced from that of $[Cp^*_3Co_3SbS_5]I$.[6] The core of this cluster consists of a distorted Co_3SbS_4 cube, with the fifth sulfur atom being inserted into one of the Sb−S edges (Chart 1). The resulting tripodal ψ-Sb(S)S ligand may be extended into the ψ-Sb(S_2)S ligand of **3** by insertion of a further sulfur atom into a second Sb−S edge.

Complex **2** crystallizes in the space group $P2_1/c$ with four formula units in the unit cell. Each asymmetric unit contains one trirhodium cluster and one disordered THF molecule. The molecular structure of **2** may also be derived from a distorted cube but with vertices occupied by three rhodium, three sulfur, and two antimony atoms. An additional sulfur atom is inserted into the Sb1−Sb2 bond. The outstanding feature of the structure is a terminal sulfur bound to Sb1 (Figure 2).

(8) Adams, R. D.; Miao, S. *Inorg. Chem.* **2005**, *358*, 1401−1406.
(9) Uchtman, V. A.; Dahl, L. F. *J. Am. Chem. Soc.* **1969**, *91*, 3756−3763.
(10) Simon, G. L.; Dahl, L. F. *J. Am. Chem. Soc.* **1973**, *95*, 2164−2174.
(11) Dobbs, D. A.; Bergman, R. G. *Inorg. Chem.* **1994**, *33*, 5329−5336.
(12) Skaugset, A. E.; Rauchfuss, T. B.; Wilson, S. R. *Organometallics* **1990**, *9*, 2875−2876.
(13) Schulz, S.; Andruh, M.; Pape, T.; Heinze, T.; Roesky, H. W.; Häming, L.; Kuhn, A.; Herbst-Irmer, R. *Organometallics* **1994**, *13*, 4004−4007.

Table 1. Selected Distances (Å) and Angles (deg) for $Cp^*_3Rh_3Sb_2S_5$ (**2**)

Rh2−Sb1	2.5670(4)	Rh3−S2	2.348(1)
Rh3−Sb1	2.5680(4)	Rh3−S3	2.411(1)
Rh1−S1	2.402(1)	Sb1−S4	2.523(1)
Rh1−S2	2.406(1)	Sb1−S5	2.297(1)
Rh1−S3	2.4007(9)	Sb2−S1	2.461(1)
Rh2−S1	2.3597(9)	Sb2−S2	2.452(1)
Rh2−S3	2.415(1)	Sb2−S4	2.366(1)
S1−Rh1−S2	88.9(1)	S4−Sb1−S5	104.2(1)
S1−Rh1−S3	82.3(1)	S1−Sb2−S2	86.6(1)
S2−Rh1−S3	82.3(1)	S1−Sb2−S4	100.6(1)
Sb1−Rh2−S1	94.2(1)	S2−Sb2−S4	100.6(1)
Sb1−Rh2−S3	77.2(1)	Rh1−S1−Rh2	97.5(1)
S1−Rh2−S3	82.8(1)	Sb2−S1−Rh1	86.9(1)
Sb1−Rh3−S2	94.0(1)	Sb2−S1−Rh2	115.8(1)
Sb1−Rh3−S3	77.3(1)	Rh1−S2−Rh3	97.2(1)
S2−Rh3−S3	83.3(1)	Rh1−S2−Sb2	87.0(1)
Rh2−Sb1−Rh3	98.0(1)	Rh3−S2−Sb2	116.4(1)
Rh2−Sb1−S4	106.1(1)	Rh1−S3−Rh2	96.1(1)
Rh2−Sb1−S5	121.3(1)	Rh1−S3−Rh3	95.7(1)
Rh3−Sb1−S4	106.4(1)	Rh2−S3−Rh3	106.8(1)
Rh3−Sb1−S5	119.6(1)	Sb1−S4−Sb2	96.2(1)

The Rh−S distances [2.348(1)−2.415(1) Å] are nearly equidistant, but the cube is slightly distorted, as expressed by angles at the vertices between 77.2(1) and 115.8(1)°. The Sb−S distances around Sb2 are comparable to those found in discrete $[SbS_3]^{3-}$ ions, i.e., $[Na(NH_3)_3]_2[Na(NH_3)_2]SbS_3$ [2.402 Å (mean)][14] and $K_3SbS_3 \cdot 3Sb_2O_3$ [2.36(1) Å].[15] Because the ionic radius of Sb(V) is smaller, the Sb−S bonds within the $[SbS_4]^{3-}$ tetrahedron in $(NH_4)_3SbS_4 \cdot 8NH_3$ [16] are still shorter (2.33 and 2.34 Å). The Sb−S distances around Sb1 in **2** (Table 1) are either very long [2.523(1) Å for Sb1−S4] or very short [2.297(1) Å for Sb1−S5].

The SbS_3 subunit is a quite common structural motif in sulfosalt chemistry, but its combination with a diatomic SbS unit is unusual.[17] The oxidation state I+ for Sb1 follows from considering the formal structural relationship between the cuboidal cluster cores of **1** and **2** (Chart 1). Replacement of one $[Cp^*Rh]^{2+}$ vertex (on the basis of closed-shell clusters, one may assume oxidation state III+ for Rh) by Sb2 (formal charge 3+) would lead to a $[Cp^*_3Rh_3SbS_5]^+$ cation. The corresponding cobalt cluster cation has already been described.[6] Further replacement of the group 16 element vertex [S2 in **1**] in the disulfide moiety by the group 15 element vertex [Sb1 in **2**] provokes an increase of positive charge. From this view, it is evident that the cluster core of **2** lacks formally two negative charges, which are gently compensated for with a strong covalent coordination of S5 at Sb1.

Such a reasoning allows one to consider the presence of an extremely electron-rich $[SSbS]^{3-}$ unit in **2**. We optimized its potential structure with density functional theory (DFT; B3LYP/3-21G hybrid functional/basis set)[18] and effectively found that the frontier HOMO and LUMO orbitals have the very high positive energies together with the very long Sb−S bonds (Table 2) equal to 2.752 Å. It clearly shows that the free $[SSbS]^{3-}$ molecule can never exist. However, this hypothetical fragment may be present in **2** by its forthcoming stabilization with positively charged Sb2, Rh2, and Rh3 atoms. Modelization of interaction of the fragment defined by S4, Sb1, and S5 with Sb2 has been performed by adding one proton to $[SSbS]^{3-}$, which leads to the $[HSSbS]^{2-}$ system. A spectacular lowering in the total energy by some 24 eV and of the frontier HOMO/LUMOs by some 5 eV is observed. However, the energies of these last molecular orbitals remain highly positive, and the optimized structure exhibits Sb−S bonds, which are shorter than those in $[SSbS]^{3-}$ but still long (2.534 and 2.880 Å; Table 2). We must comment here on the validity of the DFT calculations on the anionic species and, in particular, on why the HOMO energy for an anion is often found as positive. Cole and Perdew[19] indicated that because of the inexact nature of the exchange correlation all functionals fail to fully cancel electron−electron self-repulsion terms in the Hohenberg−Kohn−Sham DFT theorem. Consequently, it is not surprising that we find positive HOMO energies for $[SSbS]^{3-}$ and $[HSSbS]^{2-}$. However, the calculated very high positive values for our anionic models cannot be simply due to the noncanceled electron−electron repulsions and so are representative of the unstable structures of these anionic models.

In a final step of modelization, we introduced two supplementary protons on $[HSSbS]^{2-}$ potentially equivalent to the two Cp*Rh units present in **2**, giving rise to the neutral species **I**. $[HSSbH_2S]^0$ exhibits a supplementary stabilization by some 33 eV with respect to $[HSSbS]^{2-}$ and, more interestingly, the HOMO and LUMO become negative and the Δ(HOMO−LUMO) energy gap increases up to 3.8 eV. The energy gains upon the addition of protons are very high, and despite the feebleness of DFT calculations on the anions, we have here a nice demonstration of how the small unstable inorganic unit may be stabilized with organometallics. Note also that the use of hybrid functionals such as B3LYP may alleviate some electron−electron interaction, producing the negative HOMO energies for the anions.[20]

We recently calculated the Sb−S bond lengths in $[SbS]^+$, $[SbS]^0$, and $[SbS]^-$ diatomic molecules with a B3LYP/Lanl2DZ couple and found them to be equal to 2.240, 2.326, and 2.448 Å, respectively.[7] The B3LYP/3-21G functional/basis set gives the values 2.258, 2.330, and 2.438 Å, respectively, while B3LYP/3-21G* with diffuse basis set

(14) Korber, N.; Richter, F. *Helv. Chim. Acta* **2001**, *84*, 2368−2372.
(15) Graf, H. A.; Schäfer, H. *Z. Anorg. Allg. Chem.* **1975**, *414*, 220−230.
(16) Rossmeier, T.; Korber, N. *Z. Naturforsch.* **2003**, *58B*, 672−677.
(17) Wachter, J. *Angew. Chem., Int. Ed. Engl.* **1998**, *37*, 750−768.
(18) Frisch, M. J.; Trucks, G. W.; Schlegel, H. B.; Scuseria, G. E.; Robb, M. A.; Cheeseman, J. R.; Montgomery, J. A., Jr.; Vreven, T.; Kudin, K. N.; Burant, J. C.; Millam, J. M.; Iyengar, S. S.; Tomasi, J.; Barone, V.; Mennucci, B.; Cossi, M.; Scalmani, G.; Rega, N.; Petersson, G. A.; Nakatsuji, H.; Hada, M.; Ehara, M.; Toyota, K.; Fukuda, R.; Hasegawa, J.; Ishida, M.; Nakajima, T.; Honda, J.; Kitao, O.; Nakai, H.; Klene, M.; Li, X.; Knox, J. E.; Hratchian, H. P.; Cross, J. B.; Adamo, C.; Jaramillo, J.; Gomperts, R.; Stratmann, R. E.; Yazyev, O.; Austin, A. J.; Cammi, R.; Pomelli, C.; Ochterski, J. W.; Ayala, P. Y.; Morokuma, K.; Voth, G. A.; Salvador, P.; Dannenberg, J. J.; Zakrzewski, V. G.; Dapprich, S.; Daniels, A. D.; Strain, M. C.; Farkas, O.; Malick, D. K.; Rabuck, A. D.; Raghavachari, K.; Foresman, J. B.; Ortiz, J. V.; Cui, Q.; Baboul, A. G.; Clifford, S.; Cioslowski, J.; Stefanov, B. B.; Liu, G.; Liashenko, A.; Piskorz, P.; Komaromi, I.; Martin, R. L.; Fox, D. J.; Keith, T.; Al-Laham, M. A.; Peng, C. Y.; Nanayakkara, A.; Challacombe, M.; Gill, P. M. W.; Johnson, B.; Chen, W.; Wong, M. W.; Gonzalez, C.; Pople, J. A. *Gaussian 03*, Revision B.05; Gaussian, Inc.: Pittsburgh, PA, 2003.
(19) Cole, L. A.; Perdew, J. P. *Phys. Rev.* **1982**, *25*, 1265.
(20) Rienstra-Kiracofe, J. C.; Graham, D. E.; Schaefer, H. M. *Mol. Phys.* **1998**, *94*, 767.

Table 2. Distances (Å), Angles (deg), and Energy (eV) Data (B3LYP/3-21G) for $[SSbS]^{3-}$, $[HSSbS]^{2-}$, and $[HSSbH_2S]^0$ (**I**) Model Compounds

	$[SSbS]^{3-}$	$[HSSbS]^{2-}$	$[HSSbH_2S]^0$
Sb1−S4	2.752	2.880	2.542
Sb1−S5	2.752	2.534	2.339
S4−Sb1−S5	121.9	114.3	119.7
Mulliken charges S4/Sb1/S5	−1.24/−0.53/−1.24	−0.67/−0.29/−1.01	−0.36/+0.89/−0.48
E_{tot}	−192 682.451	−192 706.619	−192 739.366
E(HOMO)	+10.493	+5.759	−6.675
E(LUMO)	+12.548	+7.644	−2.863
Δ(HOMO−LUMO)	2.055	1.885	3.812

Table 3. Distances *d* (Å), Electronic Charge Density $\rho(r)$ (e/Å^3), Laplacian $\nabla^2\rho(r)$ (e/Å^5), and Total Energy Density $E_d(r)$ (Ha/Å^3) (B3LYP/3-21G*) on Local Properties for $[SSb]^+$, $[SSb]^-$, SSbCl, and $[HSSbH_2S]^0$ Model (**I**)

			SSbCl		HS4SbH$_2$S5	
	$[SbS]^+$	$[SbS]^-$	S═Sb	Sb−Cl	Sb═S5	Sb−S4H
d (Å)	2.182	2.358	2.242	2.427	2.256	2.454
$\rho(r)$	0.814	0.586	0.737	0.485	0.721	0.542
$\nabla^2\rho(r)$	5.328	2.805	3.746	3.199	1.611	1.426
$E_d(r)$	−0.406	−0.229	−0.352	−0.143	−0.353	−0.202

(usually for heavy atoms) shortens them to 2.182, 2.255, and 2.358 Å. From the valence formalism, the bond orders are equal to 3 in $[SbS]^+$, 2.5 in $[SbS]^0$, and 2 in $[SbS]^-$. However, owing to a rather high absolute electronegativity difference between Sb (4.85) and S (6.22) atoms,[21] the resonance structures with bond orders of 2, 1.5, and 1, respectively, cannot be ruled out. In agreement with these findings, the Sb2−S1, Sb2−S2, Sb2−S4, and Sb1−S4 bonds (the mean value of these four bonds is equal to 2.450 Å) in **2** may be considered as single Sb−S bonds, whereas the Sb1−S5 bond of 2.297(1) Å is rather of a double nature.

We are currently studying the topology of electron density in diatomic EX molecules and in their molybdenum and iron organometallic complexes with the AIM theory of Bader[22] and the MORPHY program of Popelier.[23] One reviewer suggested that the AIM results should be introduced to this contribution. Molina's group has done work on the topology of P−O, P−S, As−O, and As−S bonds in hypervalent phosphine and arsine oxo and thio derivatives in which a formal double E═X bond is expected.[24] They stated that the E−X bond is single and highly polarized without the contribution of d atomic orbitals of P and As. The local electronic charge densities decrease in the order P−O (1.52 e/Å^3) > As−O (1.39) > P−S (1.10) > As−S (0.88). Our preliminary results (B3LYP/3-21G*) agree with this trend. The local properties $\rho(r)$ (e/Å^3), Laplacian $\nabla^2\rho(r)$ (e/Å^5), and total energy densities $E_d(r)$ (Ha/Å^3) for $[SbS]^+$, $[SbS]^-$, SSbCl, and model **I** (Figure 3) of the Rh cluster **2** are presented in Table 3. Because the $E_d(r)$ values are negative for all compounds, the covalent nature of the bonds is proven. The properties of formal double bonds [distances *d*, $\rho(r)$, and $E_d(r)$] in S═Sb−Cl and HS−SbH$_2$═S models of **2** are intermediate between those of the $[SbS]^+$ and $[SbS]^-$ species.

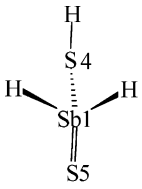

I

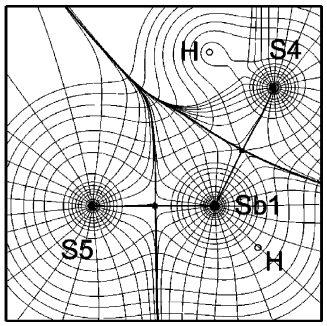

Figure 3. Gradient of electron density (ρ), interatomic surfaces (IASs), gradient paths (GPs), and (3, −1) bond critical points in the S−Sb−S plane of the model species **I**.

There are two different Sb−S bonds in model **I** (Figure 3): one single Sb−S4H and one double Sb−S5 like in the structure of **2**. The local topological properties agree with such a description. A detailed analysis of Laplacians in EX systems is currently in progress.

In conclusion, this paper provides evidence for the existence of a stable Sb═S double bond being integrated in the novel $[Sb_2S_4]^{4-}$ ligand in the trirhodium cluster **2**. The only example in which a comparatively short antimony−sulfur distance has been crystallographically determined is Ph_3SbS. This compound exhibits a Sb−S distance of 2.244(1) Å, which is still shorter than that in **2** and which was ascribed to a certain double-bond character.[25,26] The stability of the Sb−S bond in Ph_3SbS seems to be limited because it decomposes slowly in solution under loss of sulfur. Therefore, Ph_3SbS is used as a sulfur transfer reagent.[27] By contrast, **2** does not lose sulfur in hydrocarbon solutions.

Experimental Section

General Methods. All manipulations were carried out under nitrogen by Schlenk techniques. ^{1}H NMR spectra were recorded at 400 MHz. K_3SbS_3 was prepared as a yellow-brown powder in analogy to K_3AsS_3 [28] from K, S_8, and Sb_2S_3 in stoichiometric

(21) Pearson, R. G. *Inorg. Chem.* **1988**, *27*, 734−740.
(22) Bader, R. F. W. *Atoms in Molecules: a quantum theory*; Clarendon Press: Oxford, U.K., 1990.
(23) MORPHY98, a topological analysis program written by PLA Popelier with a contribution from RGA Bone (UMIST, England, EU).
(24) Dobado, J. A.; Martinez-Garcia, H.; Molina, J. M.; Sundberg, M. R. *J. Am. Chem. Soc.* **1998**, *120*, 8461−8471 and references cited therein.
(25) Weller, F.; Dehnicke, K. *Naturwissenschaften* **1981**, *68*, 523.
(26) Pebler, J.; Weller, F.; Dehnicke, K. *Z. Anorg. Allg. Chem.* **1982**, *492*, 139−147.
(27) Jason, M. E. *Inorg. Chem.* **1997**, *36*, 2641−2646.

amounts in liquid NH_3. [$Cp^*_2Rh_2Cl_4$] was prepared from $RhCl_3 \cdot 3H_2O$ and C_5Me_5H in methanol.[29]

Reaction of [$Cp_2^*Rh_2Cl_4$] with K_3SbS_3. A suspension of [$Cp_2^*Rh_2Cl_4$] (600 mg, 0.97 mmol) and K_3SbS_3 (550 mg, 1.64 mmol) in 50 mL of THF was stirred for 18 h under reflux. After cooling, the precipitate was removed by filtration and washed several times with THF. After evaporation of the solvent from the filtrate, the red-brown residue was dissolved in toluene/acetone (20:1) and chromatographed on SiO_2 (6 × 3 cm). A dark red ring was eluted with toluene/acetone (20:1) containing [$Cp^*_4Rh_4S_5$] (**1**; 55 mg, 0.05 mmol, 10%). The following weak orange band was discarded. With acetone, a dark red band was eluted containing [$Cp^*_3Rh_3Sb_2S_5$] (**2**; 52 mg, 0.05 mmol, 7%). Recrystallization of **1** from toluene at −25 °C gave red-brown prisms. **2** was recrystallized from THF at −25 °C to give dark brown rods.

In an alternative workup, the solvent was evaporated from the reaction mixture. Then the dark red-brown residue was suspended in 50 mL of Et_2O and filtered. The residue was washed with ca. 200 mL of Et_2O until the filtrate was colorless. After evaporation of the solvent from the combined solutions, the residue was dissolved in toluene/acetone (2:1) and chromatographed on SiO_2 (7 × 3 cm). With toluene/acetone (2:1), a dark red band was eluted containing **1** (127 mg, 0.11 mmol, 24%). The following band was eluted with acetone to give **2** (7 mg, 0.01 mmol, 1%).

The residue from the initial filtration was extracted with THF, evaporated to dryness, and then dissolved in 30 mL of ethanol. After filtration, the solution was combined with a solution of NH_4PF_6 (200 mg, excess) in 100 mL of water. The resulting red-brown precipitate was filtered and washed with 50 mL of H_2O and 30 mL of Et_2O. The dried precipitate was dissolved in THF, filtered again, and evaporated to dryness. The residue was dissolved in toluene/acetone (20:1) and filtered over SiO_2 (6 × 3 cm) to give a broad intensive red band of **3** (107 mg). **1**: ^{1}H NMR (300 MHz, C_6D_6, 24 °C) δ 1.81 (s, 15 H), 1.72 (s, 30 H), 1.67 (s, 15 H); FD-MS (CH_2Cl_2) *m*/*z* 1111.9 [M^+]. Anal. Found [calcd for $C_{40}H_{60}Rh_4S_5 \cdot 0.5C_7H_8$ (1158.9)]: C, 45.43 (45.08); H, 5.26 (5.57); S, 12.55 (13.83). **2**: ^{1}H NMR (300 MHz, C_6D_6) δ 1.69 (s, 30 H), 1.33 (s, 15 H); FD-MS (CH_2Cl_2) *m*/*z* 1118.2 [M^+]. Anal. Found [calcd for $C_{30}H_{45}Rh_3S_5Sb_2$ (1118.24)]: C, 34.40 (34.31); H, 4.49 (4.49); S, 13.25 (13.47). **3**: IR (KBr) $\nu(PF_6)$ 845 cm^{-1}; PI-ESI-MS (CH_3CN) *m*/*z* 1029.0 ([$Cp^*_3Rh_3SbS_6$]$^+$) (rel intens I = 100%), 997.0 ([$Cp^*_3Rh_3SbS_5$]$^+$) (I = 75%). Anal. Found [calcd for $C_{30}H_{45}F_6PRh_3S_6Sb$ (1141.45)]: C, 30.56 (30.70); H, 3.93 (3.87); S, 15.69 (16.39).

Table 4. Crystallographic Data for $C_{30}H_{45}Rh_3Sb_2S_5 \cdot C_4H_8O$ (**2**)

compd	**2**
formula	$C_{34}H_{53}ORh_3S_5Sb_2$
MW	1190.4
cryst syst	monoclinic
space group	$P2_1/c$
a, Å	10.0804(5)
b, Å	18.5111(10)
c, Å	21.9383(11)
β, deg	95.44(1)
V, Å^3	4075.3(4)
Z	4
d_{calc}, g/cm^3	1.940
F(000)	2328
cryst size, mm^3	0.36 × 0.14 × 0.08
diffractometer	STOE-IPDS
T, K	173
θ, deg	1.86−25.82
no. of reflns collected	39 686
no. of indep reflns	7835
R_{int}	0.0676
no. of obsd reflns	6227 ($I > 4\sigma$)
μ, mm^{-1}	2.780
no. of param	402
GOF on F^2	0.919
abs correction	numerical
T_{max}, T_{min}	0.7535, 0.3535
R1, wR2 ($I > 2\sigma$)	0.0271, 0.0594
R1, wR2 (all data)	0.0390, 0.0615

Crystal Structure Determination of $Cp^*Rh_3Sb_2S_5 \cdot C_4H_8O$ (2). A dark brown plate of dimensions 0.36 × 0.14 × 0.08 mm was used for data collection on a Stoe-IPDS diffractometer (Mo Kα radiation, graphite monochromator). Crystallographic details are given in Table 4. The structure was solved by direct methods and refined by full-matrix least-squares (SHELXL97 program) with all reflections. All non-hydrogen atoms were refined with anisotropic displacement parameters, the H atoms were calculated geometrically, and a riding model was used during the refinement process. A solvent molecule (THF) is located on an inversion center, and it is disordered. Two positions have been calculated, taking into account the electron density of the hole.

Acknowledgment. We gratefully acknowledge Prof. Dr. H. Brunner for continuous support.

Supporting Information Available: Two X-ray crystallographic files, in CIF format. This material is available free of charge via the Internet at http://pubs.acs.org.

IC050493E

(28) Kanatzidis, M. G.; Chou, J. H. *J. Solid State Chem.* **1996**, *127*, 186−201.

(29) (a) Bauer, C. Thesis, University of Regensburg, Regensburg, Germany, 1983; p 216. (b) White, C.; Yates, A.; Maitlis, P. M. *Inorg. Synth.* **1992**, *29*, 228−230.